



	Experiment title: Sub-micron-diffraction and fluorescence analysis of InGaAlAs/InGaAlAs multi quantum well heterostructures by Selective Area Growth	Experiment number: HS-4020
Beamline: ID-01	Date of experiment: from: 02-march-2010 to: 08-march-2010	Date of report: 22/07/2010
Shifts:	Local contact(s): Gerardina Carbone	<i>Received at ESRF:</i>

Names and affiliations of applicants (* indicates experimentalists):

Jean Décobert : AT III-V Lab

Ronan Guillamet : AT III-V Lab

Cristian Mocuta : Synchrotron SOLEIL

Olivier Patard : AT III-V Lab

Report:

Alcatel Thales III-V Lab is performing advanced research on optical sources (lasers) for fiber optic telecommunications at 10-40 Gb/s. Many efforts are done to simultaneously increase the device performances and to reduce their size, consumption and cost. To achieve this goal, the most attractive way is to **integrate** individual photonic functions as close as possible one to each other on the same wafer. **Metal-organic vapor phase epitaxy (MOVPE)** in the regime of **selective area growth (SAG)** is the advanced technology platform for integrated optoelectronic devices made of GaInAsP or AlGaInAs **multiple quantum well (MQW)** structures on InP substrates.

SAG consists in growing III-V semi-conductor materials on partially masked substrates. The SAG masks consist of symmetric pairs of SiO₂ stripes deposited on the substrate prior to the growth. As no deposition occurs on the amorphous surface of the dielectric mask, a concentration gradient builds up in the vapor phase, that locally enhance the growth in the short vicinity of the dielectric mask (fig.1). As a consequence, after the epitaxial growth, the thicknesses are non-uniform with respect to the mask position. Furthermore, as the different species have different diffusion lengths in the gas phase, compositional changes could be observed as well. The main interest is to determine the optimal mask pattern (through computational simulations) and SAG conditions to obtain perfect quality of the MQW-based optoelectronic light-emitting components. Due to the restricted dimension and property changes of the area of interest, a local-probe technique, **microbeam x-ray diffraction (μ -XRD)** mapping, has been used for characterization at ID-01 beamline.

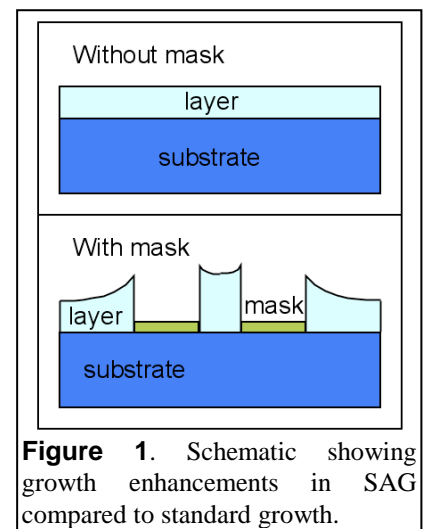


Figure 1. Schematic showing growth enhancements in SAG compared to standard growth.

The X-ray focusing element consists of a Au-made 200 μ m diameter Fresnel Zone Plate (FZP), having the last zone width $\Delta r_n = 100$ nm. At a beam energy $E = 8$ keV a focal distance of ~ 130 mm was found. The cleanliness of the focused spot was ensured by the use of a 60 μ m beamstop placed upstream and an Order Sorting Aperture (OSA, 50 μ m pin-hole) placed downstream the FZP. The resulting X-ray spot was measured with a knife edge and found to be of $0.5 \times 0.5 \mu\text{m}^2$ size, size also confirmed furtherer during the measurements (*e.g.* when crossing sharp sample edges). By reducing the illuminated area of the FZP, we can tune the vertical divergence of the beam; a value of 14×10^{-3} degrees was found, mesured from the width of

the rocking curve of the substrate (assimilated to a ‘perfect’ crystal, of natural width ~few mdeg.). A photon flux of 1.3×10^7 ph/s. was measured in the focused x-ray spot.

The sample is placed on a diffractometer dedicated for microbeam studies, allowing all the degrees of freedom required for such experiments (accurate angles and lateral translations for positioning the sample into the small beam, accurate diffraction angles). Most of the measurements were performed around an incident angle $\theta \sim 30^\circ$, yielding thus to a beam footprint on the sample of $\sim 0.5 \times 1 \mu\text{m}^2$ (FWHM, horizontal \times vertical), which will constitute the lateral resolution achieved during this experiment. In order to find the area(s) of interest, the sample is roughly positionned (within several $10 \mu\text{m}$) using an optical microscope aligned to the reference position of the microbeam. With the angles of the diffractometer set to values characteristic of the sample (*e.g.* corresponding to the Bragg angles of the layers constituting the sample), the lateral position of the sample is scanned while recording the intensity in the detector in each point. The result is a map allowing to position the regions of interest into the beam. Then the angles are varied in order to map (with high resolution) the diffraction signal - this is possible with the adapted μXRD setup allowing such movements without changing the illuminated area on the sample.

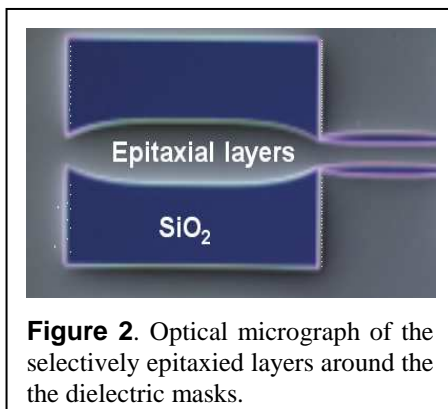


Figure 2. Optical micrograph of the selectively epitaxiated layers around the dielectric masks.

In the following, we will detail some examples of the studies performed. Twelve samples made of different heterostructures deposited on InP or GaAs substrates were analyzed during the allocated beamtime. Each sample had complex and different mask pattern areas (see *e.g.* fig. 2). Depending on the sample, from 3 and up to 15 different SAG areas (epitaxial structures) were analyzed on the same chip by performing high resolution XRD measurement along the specular direction (θ - 2θ scans). Thickness, composition and strain variations of the quantum well and barrier materials in the narrow opening width were extracted through the measurements. The spatial resolution was determined essentially by the beam size. This very little spot size has allowed recording different cross

sections through the opened area (with lateral steps of $1 \mu\text{m}$). Several cross sections were also acquired when moving from the edge of the mask toward the field area, far from the mask influence. Figure 3 shows tenths of θ - 2θ curves acquired step by step in the x direction. The sample is made of strain compensated $\text{Al}_x\text{Ga}_{1-x}\text{As}$ MQWs. As the mask influence decreases, the thickness decreases as well (larger period of the satellites) and the aluminum and gallium concentration increases, due to their higher diffusion lengths compared to that of indium (satellites shift toward tensile strain).

In view of new device conception and optimization, computational modelling is absolutely necessary to design properly the mask (form and position) and to prepare the material growth sequence, in order to obtain everywhere the required heterostructures. The data obtained through the experiments at ID-01 have permitted not only accurate characterization at the micron scale, but also precise **model refining** and **model validation** of the related phenomena. Indeed, one of the objectives of the project was to measure the vapor phase diffusion length (D/k) parameters for the three Al, Ga and In precursors, D and k being the diffusion and sticking coefficient respectively of the different species. Despite a numerous literature over the last ten years about μXRD applied on SAG of III-V material, little is known about D/k for Al precursor of SAG of MQW structures with the three group-III elements (Al, Ga and In).

We report here the two main results obtained during the experiment HS-4020, taken among numerous data.

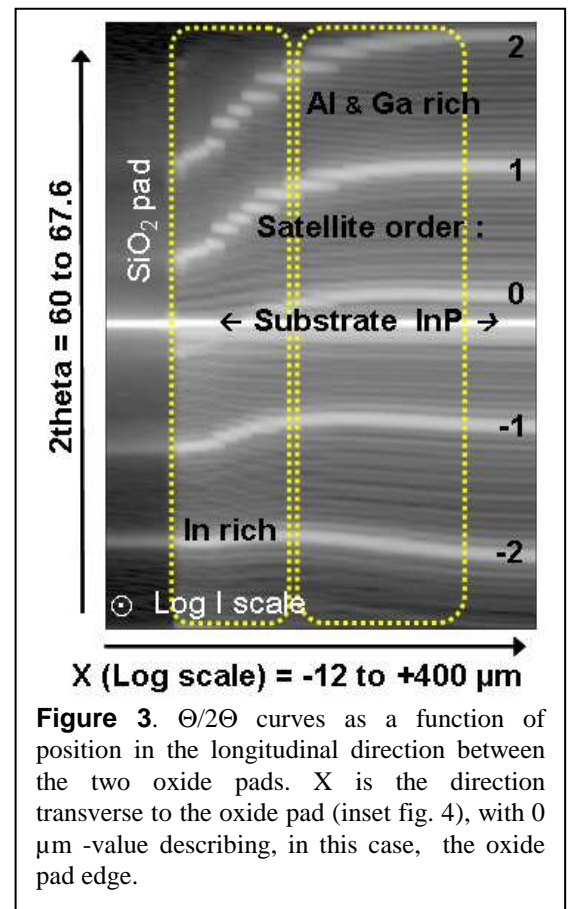
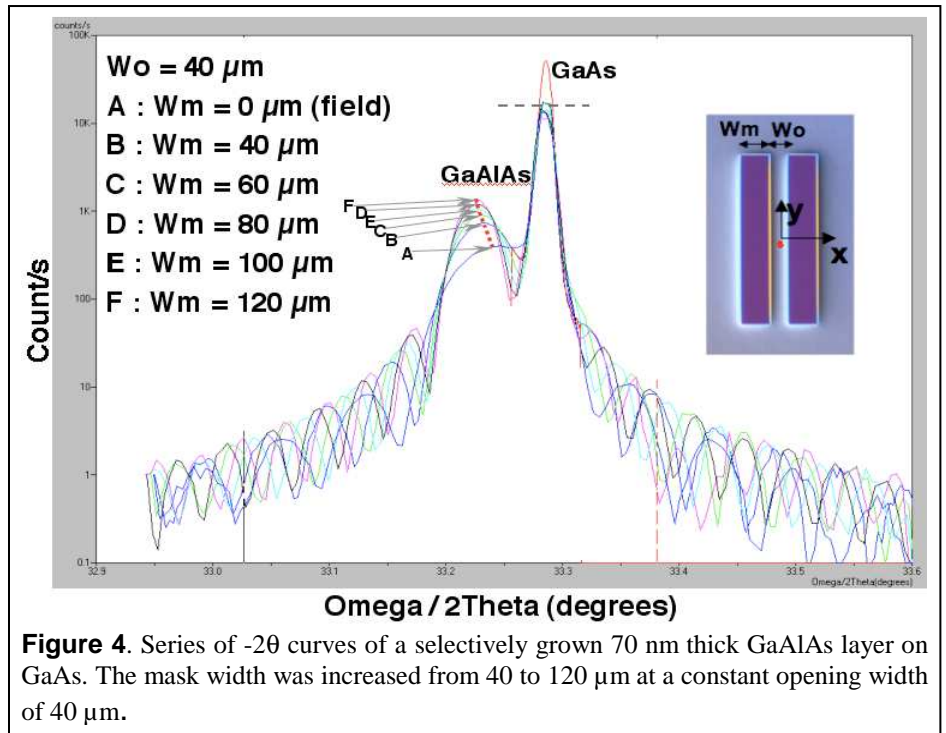


Figure 3. $\theta/2\theta$ curves as a function of position in the longitudinal direction between the two oxide pads. X is the direction transverse to the oxide pad (inset fig. 4), with 0 μm -value describing, in this case, the oxide pad edge.

The first one is, for the first time, the extraction of the D/k value for aluminum precursor. To obtain this value, a 70 nm thick GaAlAs layer selectively grown on GaAs was characterized by a series of micro-diffraction scans (fig. 4). The mask width was increased from 40 to 120 μm at a constant opening width of 40 μm . Each scan was measured at the center of the gap except the first one, which was taken in the reference area (field). One can see the progressive shift of the layer peak toward higher Al concentration, (even if very weak, due to the quasi identical lattice parameter of AlAs and GaAs binary materials). This indicates lower diffusion length for Al compared to Ga. In our growth conditions, the values were 50 μm and 85 μm for Al and Ga respectively. Future work will be done in order to follow this parameter as a function of growth parameters (such as pressure or temperature).



The second main result was obtained on AlGaInAs/AlGaInAs periodic structures. First and as expected, we observed that indium, which has the shortest effective diffusion length, highly enriches in the near vicinity of the mask compared to the reference area, far from the mask. This leads to a red shift of the material wavelength emission. On the other hand, the other elements, aluminum and gallium, with a higher diffusion length, have an influence which extends further from the mask edge (fig. 3). This long-range effect of Al and Ga is particularly enhanced in the high mask density scheme of our samples. Due to neighbor mask cell's influence, a non-negligible Al and Ga enrichment occurs between the different masks which correspond now to a blue shift of the material wavelength emission. The systematic measurements performed in 4 predefined areas of the samples have allowed quantifying this phenomenon. This has brought new data to further refine the vapor phase diffusion SAG modeling for the AlGaInAs system. Composition variations were higher than expected and predicted by the model. This abnormal behavior, even if in qualitative agreement, is still under investigation. A possible reason would be that the SAG of very thin layers (less than 10 nm) is much more sensitive to transient sequences between the stacked layers than to thick bulk material. The hypothesis is that the higher concentration of elements from group III over the oxide pads acts as a reservoir to supply extra and unpredicted material during growth interruptions. Special samples are being grown to further analyze this behavior and validate this hypothesis.

These results (D/k value of Al, long-range effect of Al and Ga), among others achieved during the same shifts, are reported for the first time on AlGaInAs material family. They will be presented at the JNMO (Journée Nationale de Micro- et Opto-électronique) in October this year. A paper in preparation will be soon submitted to Applied Physics Letters.

The next step is now to take advantage of the validated setup and the calibrated simulation tool to investigate much more complex heterostructures as they are used in advanced MQW based optoelectronic devices.